

A Spatio-Temporal Point Process Model for Ambulance Demand

Zhengyi Zhou, David S. Matteson, Dawn B. Woodard,
Shane G. Henderson and Athanasios C. Micheas*

December 3, 2014

Abstract

We introduce a parsimonious Bayesian approach for modeling spatio-temporal point processes. Our method is motivated by the problem of estimating the spatial distribution of ambulance demand in Toronto, Canada, as it changes over discrete 2-hour intervals; such estimates are critical for fleet management and dynamic deployment. The large-scale datasets typical in ambulance demand estimation exhibit complex spatial and temporal patterns and dynamics. We propose to model this time series of spatial densities by finite Gaussian mixture models. We fix the mixture component distributions across all time periods while letting the mixture weights evolve over time. This allows efficient estimation of the underlying spatial structure, yet enough flexibility to capture dynamics over time. We capture temporal patterns such as seasonality by introducing constraints on the mixture weights; we represent location-specific temporal dynamics by applying a separate autoregressive prior on each mixture weight. While estimation may be performed using a fixed number of mixture components, we also extend to estimate the number of components using birth-and-death Markov chain Monte Carlo. We quantify statistical and operational merits of our method over the current industry practice.

KEY WORDS: Non-homogeneous Poisson point process; Gaussian mixture model; Markov chain Monte Carlo; Autoregressive prior; Emergency medical services.

Short title: Spatio-Temporal Ambulance Demand

*Zhou is a PhD Candidate at the Center for Applied Mathematics, Cornell University, 657 Rhodes Hall, Ithaca, NY 14853 (E-mail: zz254@cornell.edu, webpage: <http://www.cam.cornell.edu/~zz254/>). Matteson is an Assistant Professor at the Department of Statistical Science, Cornell University, 1196 Comstock Hall, Ithaca, NY 14853 (Webpage: <http://www.stat.cornell.edu/~matteson/>). Woodard is an Assistant Professor at the School of Operations Research and Information Engineering, Cornell University, 228 Rhodes Hall, Ithaca, NY 14853 (Webpage: <http://people.orie.cornell.edu/woodard/>). Henderson is a Professor at the School of Operations Research and Information Engineering, Cornell University, 230 Rhodes Hall, Ithaca, NY 14853 (Webpage: <http://people.orie.cornell.edu/shane/>). Micheas is an Associate Professor at the Department of Statistics, 134G Middlebush Hall, University of Missouri-Columbia, Columbia, MO 65203 (Webpage: <http://www.stat.missouri.edu/~amicheas/>).

1 Introduction

This article describes an efficient and flexible method to model a time series of spatial densities. Our motivating application is estimating ambulance demand over space and time in Toronto, Canada. Emergency medical service (EMS) managers need accurate demand estimates to minimize response times to emergencies and keep operational costs low. These demand estimates are typically required at least for every four-hour work shift, and at very fine spatial resolutions for fine-grained dynamic deployment planning. We propose a method to model ambulance demand continuously on the spatial domain, as it changes over every two-hour interval.

Several studies have modeled aggregate ambulance demand as a temporal process, using autoregressive moving-average models (Channouf et al., 2007), dynamic latent factor structure (Matteson et al., 2011) or singular spectrum analysis (Vile et al., 2012). While these temporal estimates inform staffing and fleet size, spatio-temporal demand estimates are critical for selection of base locations and for dynamic deployment planning, but have received far less attention. Current industry practice for spatial-temporal demand forecasting usually uses a simple averaging technique over a discretized spatial and temporal domain; the demand estimate for a small spatial region in a particular time period is taken to be the average of several historical demand values for the same region during corresponding periods in previous weeks or years. Averages of so few data points can produce noisy estimates, and can vary greatly with changes in the discretization. Setzler et al. (2009) use artificial neural networks (ANN) on discretized spatial and temporal domains, and compare it to industry practice. ANN is superior at low spatial granularity, but both methods produce noisy results at high spatial resolutions. Our method is suitable for estimation on very fine scales in time and space.

We use data from Toronto Emergency Medical Services, for February 2007, and evaluate out-of-sample performance on data from March 2007 and February 2008. Our data consist of 45,730 priority emergency events received by Toronto EMS for which an ambulance was dispatched. Each record contains the time and the location to which the ambulance was dispatched. Figure 1 shows all observations from the training data (February 2007) and explores some temporal characteristics at downtown Toronto. For each two-hour period, we compute the proportion of

observations that arise from the downtown region (outlined by the rectangle) out of all observations from that period. We analyze the autocorrelation of the time series of proportions in Figure 1(b). We observe evidence for weekly (84 time periods) and daily (12 time periods) seasonality as well as low-order autocorrelation (dashed lines represent approximate 95% confidence interval). Upon analyzing other localities, we consistently found weekly seasonality, but daily seasonality and low-order autocorrelation tend to be stronger at locations such as downtown or dense residential regions, and weaker at others such as dispersed residential areas or large parks.

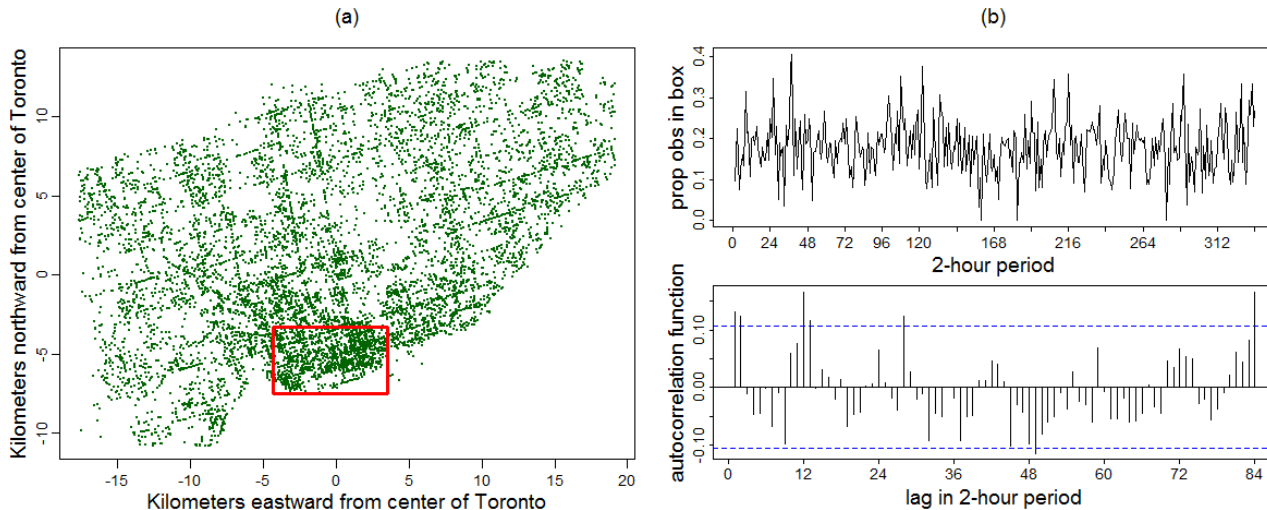


Figure 1: (a) all 15,393 observations in the training data (February 2007), with downtown subregion outlined by a rectangle; (b) time series (top) and autocorrelation function (bottom) of the proportions of observations arising from the rectangle across two-hour periods. Weekly, daily seasonality and low-order autocorrelation are observed.

There are several challenges to our modeling problem. First, the number of observations per two-hour period is low (average is 45); this makes it difficult to estimate the spatial structure at each time period. Second, we need to capture the set of complex, location-specific temporal patterns and dynamics in the point process. Third, computation can be difficult given the large amount of data and large number of time periods.

Spatial point processes have frequently been modeled using non-homogeneous Poisson processes (NHPP) (Diggle, 2003; Møller and Waagepetersen, 2004; Illian et al., 2008). In particular, Bayesian semiparametric mixture modeling has been proposed to account for heterogeneity in the

spatial density. Examples of this approach include Dirichlet processes with beta or normal densities (Kottas and Sansó, 2007; Ji et al., 2009), and finite Gaussian mixture models with a fixed number of components (Chakraborty and Gelfand, 2010). Spatial mixture modeling has been extended to spatio-temporal settings via dependent Dirichlet process mixture models (Taddy, 2010; Ding et al., 2012; Taddy and Kottas, 2012). These methods allow the stick-breaking weights of the Dirichlet process to evolve in an autoregressive manner, but necessitates a simple first-order dependence structure common to all components. Extending such a method to include higher-order serial dependence and seasonality effects is not entirely straightforward. These dependencies could be made location-specific by discretizing the spatial domain into sub-regions and imposing a different autoregressive parameter for each region. Such an implementation is sensitive to spatial partitioning, and it adds substantial computational complexity.

To address our modeling aims, we introduce a novel class of finite mixture models. We assume a common set of mixture components across time periods, to promote effective learning of the spatial structure across time, and to overcome sparsity of data at each period. We allow the mixture weights to vary over time; we capture temporal patterns and dynamics in the spatial density by imposing seasonal constraints and applying autoregressive priors on the mixture weights. The number of mixture components may be fixed or estimated via birth-and-death Markov chain Monte Carlo (Stephens, 2000). We compare our method with a current industry practice and an extension of this industry practice. Our method is shown to have highest statistical predictive accuracy, as well as the least error in measuring operational performance.

We define the general setting and propose our mixture model using a fixed number of components in Section 2. We extend our mixture model to estimate the number of components in Section 3. We show the results of estimating ambulance demand in Toronto in Section 4, and assess the performance and validity of our approach in Section 5. Section 6 concludes.

2 Spatio-Temporal Finite Mixture Modeling

We investigate Toronto’s ambulance demand on a continuous spatial domain $\mathcal{S} \subseteq \mathbb{R}^2$ and a discretized temporal domain $\mathcal{T} = \{1, 2, \dots, T\}$ of two-hour intervals ($T = 336$ for 28 days in

February 2007). Our method extends trivially to any spatial domain with higher dimensions.

Let $\mathbf{s}_{t,i}$ denote the spatial location of the i th ambulance demand occurring in the t -th time period, for $i \in \{1, \dots, n_t\}$. We assume that the set of spatial locations in each time period independently follows a non-homogeneous Poisson point process over \mathcal{S} with positive integrable intensity function λ_t . The intensity function for each period t can be decomposed as $\lambda_t(\mathbf{s}) = \delta_t f_t(\mathbf{s})$ for $\mathbf{s} \in \mathcal{S}$, in which $\delta_t = \int_{\mathcal{S}} \lambda_t(\mathbf{s}) d\mathbf{s}$ is the aggregate demand intensity for period t , and $f_t(\mathbf{s})$ is the spatial density of demand in period t , i.e., $f_t(\mathbf{s}) > 0$ for $\mathbf{s} \in \mathcal{S}$ and $\int_{\mathcal{S}} f_t(\mathbf{s}) d\mathbf{s} = 1$. Then we have $n_t | \lambda_t \sim \text{Poisson}(\delta_t)$ and $\mathbf{s}_{t,i} | \lambda_t, n_t \stackrel{iid}{\sim} f_t(\mathbf{s})$ for $i \in \{1, \dots, n_t\}$.

We assume that $\{\delta_t\}$ is known or can be obtained from temporal aggregate demand studies such as Channouf et al. (2007). Here we focus on modeling the spatial densities $\{f_t(\mathbf{s})\}$ using Gaussian mixture models. We build our model in three steps. We first introduce in Section 2.1 our general framework of mixture models with common component distributions across time. We add constraints on the mixture weights in Section 2.2 to describe weekly seasonality. We also place autoregressive priors on the mixture weights to capture location-specific dependencies in Section 2.3. Finally, the computational methods are described in Section 2.4. For now, we fix the number of mixture components, K ; we incorporate estimation of K in Section 3.

2.1 A Spatio-Temporal Gaussian Mixture Model

We consider a bivariate Gaussian mixture model in which the component distributions are common through time, while mixture weights change over time. Fixing the component distributions allows for information sharing across time to build an accurate spatial structure, because each time period typically has few observations. It is also natural in our application, which has established hotspots such as downtown, residential areas and central traffic routes. Letting the mixture weights vary across time enables us to capture dynamics in population movements and actions at different locations and times. Our methods can be trivially extended to other distribution choices such as a mixture of Student's t distributions. For any $t \in \mathcal{T}$, we model the

spatial distribution by a K -component Gaussian mixture

$$f_t(\mathbf{s}; \{p_{t,j}\}, \{\boldsymbol{\mu}_j\}, \{\boldsymbol{\Sigma}_j\}) = \sum_{j=1}^K p_{t,j} \phi(\mathbf{s}; \boldsymbol{\mu}_j, \boldsymbol{\Sigma}_j), \quad \forall \mathbf{s} \in \mathcal{S}, \quad (1)$$

in which ϕ is the bivariate Gaussian density, with mean $\boldsymbol{\mu}_j$ and covariance matrix $\boldsymbol{\Sigma}_j$, for $j \in \{1, \dots, K\}$. The mixture weights are $\{p_{t,j}\}$, satisfying $p_{t,j} \geq 0$ and $\sum_{j=1}^K p_{t,j} = 1$ for all t and j . The component means and covariances are the same in all time periods; only the mixture weights are time-dependent.

2.2 Modeling Seasonality with Constraints

We observe weekly seasonality in ambulance demand across the spatial domain (Section 1). We represent this weekly seasonality by constraining all time periods with the same position within a week (e.g., all periods corresponding to Monday 8-10am) to have common mixture weights.

Let $B \in \mathbb{N}$ ($B \ll T$) denote a time block, corresponding to the desired cycle length. In our application, $B = 84$, the number of 2-hour periods in a week. Each $t \in \mathcal{T}$ is matched to the value of $b \in \{1, \dots, B\}$ such that $b \bmod B = t \bmod B$. We modify Equation (1) to

$$f_t(\mathbf{s}; \{p_{t,j}\}, \{\boldsymbol{\mu}_j\}, \{\boldsymbol{\Sigma}_j\}) = f_b(\mathbf{s}; \{p_{b,j}\}, \{\boldsymbol{\mu}_j\}, \{\boldsymbol{\Sigma}_j\}) = \sum_{j=1}^K p_{b,j} \phi(\mathbf{s}; \boldsymbol{\mu}_j, \boldsymbol{\Sigma}_j), \quad (2)$$

so that all periods with the same position within the cycle have the same set of mixture weights.

The usefulness of such constraints on mixture weights is not limited to representing seasonality. We can also exempt special times, such as holidays, from seasonality constraints, or combine consecutive time periods with similar characteristics, such as rush hours or midnight hours.

2.3 Autoregressive Priors

We also observe that EMS demand exhibits low-order serial dependence and daily seasonality whose strengths vary with locations (Section 1). We can capture this in our mixture model by placing a separate autoregressive prior on each time series of mixture weights, i.e., on $\{p_{b,j}\}_{b=1}^B$ for each j in Equation (2). Such autoregressive priors are widely used in spatial data to encourage similar parameter estimates at neighboring locations (Besag et al., 1991), and in temporal

processes to smooth parameter estimates from adjacent times (Knorr-Held and Besag, 1998).

With such priors, we can represent a rich set of dependence structures, including complex seasonality and high-order dependence structures, which may be especially helpful for analyzing temporal patterns across fine time scales. We can also use unique specification and parameters for each mixture weight, allowing us to detect location-specific temporal patterns.

The mixture weights, $p_{b,j}$, are subject to nonnegativity and sum-to-unity constraints; placing autoregressive priors and manipulating them would require special attention. Instead, we transform them to an unconstrained parametrization via multinomial logit transformation

$$\pi_{b,r} = \log \left[\frac{p_{b,r}}{1 - \sum_{j=1}^{K-1} p_{b,j}} \right], \quad r \in \{1, \dots, K-1\}. \quad (3)$$

We then specify autoregressive priors on the transformed weights $\{\pi_{b,r}\}$. For our application, we use the autoregressive priors to capture first-order autocorrelation and daily seasonality.

We assume that the de-measured transformed weights from any time period depend most closely on those from four other time periods: immediately before and after (to represent short-term serial dependence), and exactly one day before and after (to capture daily seasonality). We impose the following priors

$$\begin{aligned} \pi_{b,r} | \boldsymbol{\pi}_{-b,r} &\sim N \left(c_r + \rho_r [(\pi_{b-1,r} - c_r) + (\pi_{b+1,r} - c_r) + (\pi_{b-d,r} - c_r) + (\pi_{b+d,r} - c_r)], \nu_r^2 \right), \\ c_r &\sim N(0, 10^4), \quad \rho_r \sim U(0, 0.25), \quad \nu_r^2 \sim U(0, 10^4), \end{aligned} \quad (4)$$

for $r \in \{1, \dots, K-1\}$ and $b \in \{1, \dots, B\}$, in which $\boldsymbol{\pi}_{-b,r} = (\pi_{1,r}, \dots, \pi_{b-1,r}, \pi_{b+1,r}, \dots, \pi_{B,r})$, and d is the number of time periods in a day ($d = 12$ in our case). Since every week has the same sequence of spatial densities, we define priors of $\{\pi_{b,r}\}$ circularly in time, such that the last time period is joined with the first time period. In the prior specification of $\{\pi_{b,r}\}$, the autoregressive parameters ρ_r determine the persistence in the transformed mixture weights over time, while the intercepts c_r determine their mean levels, and the variances ν_r^2 determine the conditional variability. These three parameters are component-specific, and therefore location-specific. For any $\rho_r \in (-0.25, 0.25)$, the joint prior distribution of $[\pi_{1,r}, \dots, \pi_{B,r}]$ is a proper multivariate normal distribution (Besag, 1974); we take the priors of ρ_r to be $U(0, 0.25)$ because exploratory data analysis only detected evidence of nonnegative serial dependence. The priors on c_r and

ν_r are diffuse, reflecting the fact that we have little prior information regarding their values.. Alternatively to this circular definition of mixture weights with symmetric dependence on past and future, one can also specify the marginal distribution of $\pi_{1,r}$ and let each $\pi_{b,r}$ depend only on its past. In either setting, we can represent a wide range of complex temporal patterns.

2.4 Bayesian Estimation

We apply Bayesian estimation, largely following Richardson and Green (1997) and Stephens (2000) in our choices of prior distributions and hyperparameters. Richardson and Green (1997) define a set of independent, weakly informative and hierarchical priors conjugate to univariate Gaussian mixture models, which Stephens (2000) extends to the multivariate case. We extend to incorporate time-varying mixture weights, and instead of imposing independent Dirichlet priors on $\{p_{b,j}\}$, we impose autoregressive priors on $\pi_{b,r}$ as in (4). For all other parameters, we have for $j \in \{1, \dots, K\}$ and $t \in \{1, \dots, T\}$,

$$\begin{aligned} \boldsymbol{\mu}_j &\sim \text{Normal}(\boldsymbol{\xi}, \boldsymbol{\kappa}^{-1}), & \boldsymbol{\Sigma}_j^{-1} | \boldsymbol{\beta} &\sim \text{Wishart}(2\alpha, (2\boldsymbol{\beta})^{-1}), \\ & & \boldsymbol{\beta} &\sim \text{Wishart}(2g, (2\mathbf{h})^{-1}), \end{aligned} \tag{5}$$

in which we set $\alpha = 3$, $g = 1$ and

$$\boldsymbol{\xi} = \begin{bmatrix} \xi_1 \\ \xi_2 \end{bmatrix}, \quad \boldsymbol{\kappa} = \begin{bmatrix} \frac{1}{R_1^2} & 0 \\ 0 & \frac{1}{R_2^2} \end{bmatrix}, \quad \mathbf{h} = \begin{bmatrix} \frac{10}{R_1^2} & 0 \\ 0 & \frac{10}{R_2^2} \end{bmatrix},$$

in which ξ_1 and ξ_2 are the medians of all observations in the first and second spatial dimensions, respectively, and R_1 and R_2 are the lengths of the ranges of observations in the first and second spatial dimensions, respectively. The prior on each $\boldsymbol{\mu}_j$ is diffuse, with prior standard deviation in each spatial dimension equal to the length of the range of the observations in that dimension. The inverse covariance matrices $\boldsymbol{\Sigma}_j^{-1}$ are allowed to vary across j , while centering around the common value $E(\boldsymbol{\Sigma}_j^{-1} | \boldsymbol{\beta}) = \alpha \boldsymbol{\beta}^{-1}$. The constant α controls the spread of the priors on $\boldsymbol{\Sigma}_j^{-1}$; this is taken to be 3 as in Stephens (2000), yielding a diffuse prior for $\boldsymbol{\Sigma}_j^{-1}$. The centering matrix $\boldsymbol{\beta}^{-1}$ is given an even more diffuse prior, by since g is taken to be a smaller positive constant. Our choice of \mathbf{h} is the same as Stephens (2000).

We do computation via Markov chain Monte Carlo (MCMC). We augment each observation

$\mathbf{s}_{t,i}$ with its latent component label $z_{t,i}$, simulating a Markov chain with limiting distribution equal to the joint posterior distribution of $\{z_{t,i}\}$, $\{\boldsymbol{\mu}_j\}$, $\boldsymbol{\beta}$, $\{\boldsymbol{\Sigma}_j\}$, $\{\pi_{b,r}\}$, $\{c_r\}$, $\{\rho_r\}$, and $\{\nu_r\}$. We update $\{z_{t,i}\}$, $\{\boldsymbol{\mu}_j\}$, $\boldsymbol{\beta}$ and $\{\boldsymbol{\Sigma}_j\}$ by their closed-form full conditional distributions, and update $\{\pi_{b,r}\}$, $\{c_r\}$, $\{\rho_r\}$ and $\{\nu_r\}$ via random-walk Metropolis-Hastings.

3 Estimating the Number of Components

We assumed a fixed number of mixture components in developing our model in Section 2; in this section, we estimate a variable number of components. Allowing the number of components to vary typically improves the mixing (efficiency) of the MCMC computational method, by allowing the Markov chain to escape local modes more quickly. We adapt the birth-and-death MCMC (BDMCMC) computational method from Stephens (2000) to a spatio-temporal setting.

Each iteration of Stephens’ BDMCMC is a two-stage process. In the first stage, new components are “born” or existing ones “die” in continuous time. Parameters of new-born components are sampled from their respective priors. Components die at a rate so as to maintain sampling stationarity; they die according to their relative implausibility as computed from the likelihood of data and priors. After each birth or death, the mixture weights are scaled proportionally to maintain sum-to-one invariance within each time period. After a fixed duration of births and deaths, in the second stage, the number of components are fixed and distributional parameters and mixture weights of the components are updated using full conditionals or Metropolis-Hastings.

We can generalize Stephens’ BDMCMC to incorporate time-varying mixture weights in a straightforward way, by maintaining the same number of components across different time periods within each iteration. Since the birth and death process applies in the same way to all time periods, it is easy to show that stationarity holds for this generalized sampling method. Following Stephens (2000), we assume a truncated Poisson prior on the number of components ℓ , i.e., $P(\ell) \propto \tau^\ell / \ell!$, $\ell \in \{1, \dots, \ell_{max}\}$ for some fixed τ and ℓ_{max} . All other priors and hyperparameters are as specified in (4) and (5), and the spatial density function at each time is as in (2).

4 Estimating Ambulance Demand

We fit our full Gaussian mixture model with seasonality constraints and autoregressive priors (Section 2) on the Toronto EMS data from February 2007. First, we use a fixed number of 15 components. We found 15 components to be large enough to capture a wide range of residential, business and transportation regions in Toronto, yet small enough for computational ease given the large size of the dataset. We then fit the model again with a variable number of components (Section 3). We set the *a priori* maximum number of components $\ell_{max} = 50$ and choose the prior mean of the number of components, τ , such that the posterior average numbers of components are 19 or 24 (posterior standard deviations are 3.1 and 4.6, respectively). Given the large amount of data and the complexity of our method, imposing a vague prior on the number of components would result in an unfeasibly large number of mixture components, and may lead to overfitting.

Each MCMC algorithm is run for 50,000 iterations, with the first 25,000 iterations discarded as burn-in. In Section 5.2 we report the estimated MCMC standard errors of our performance measures (Flegal et al., 2008); they are small enough to provide accuracy to 3 significant figures, indicating satisfactory chain length and mixing. Using a personal computer, the computation times for our model with 15 components is about 4 seconds per iteration, compared to 7 and 8 seconds using variable numbers of components averaged 19 and 24, respectively. In practice, estimation using our model only needs to be performed infrequently (at most once a month in our application); density prediction of any future time period can then be immediately calculated as the corresponding density using the most recent parameter estimation results.

Figure 2 presents results from fitting using 15 components. It shows the ellipses at the 90% level associated with each of the 15 components, using the parameter values from the 50,000th iteration of the Markov chain. The ellipse for each component is shaded by the posterior mean of ρ_r for that component, except for the 15th component because $r \in \{1, \dots, 14\}$. Components at the denser greater downtown and coastal regions of Toronto have the highest estimates of ρ_r ; these regions exhibit the strongest low-order serial dependence and daily seasonality. Our model is able to easily differentiate temporal patterns and dynamics at different locations.

Figure 3 show posterior log spatial densities at Wednesday around midday and midnight as

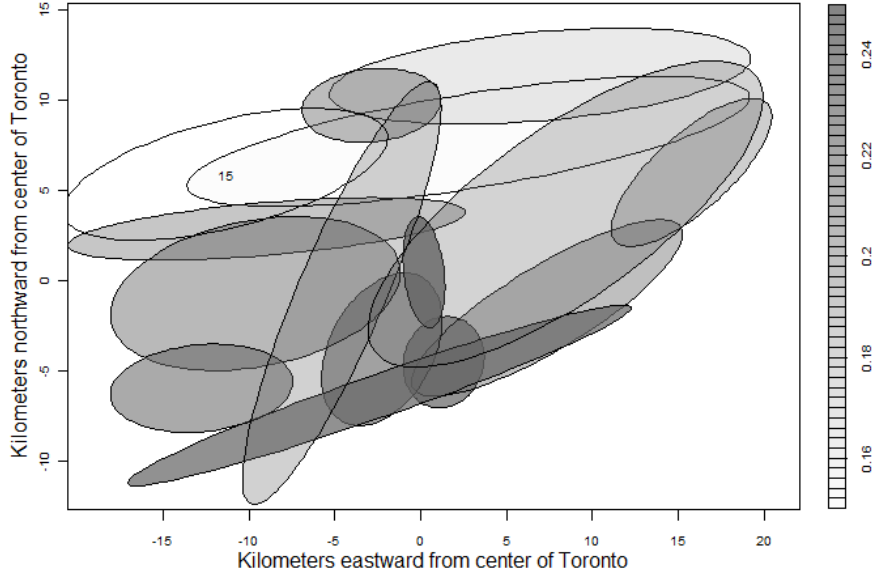


Figure 2: Ellipses at the 90% level for all components, when fitting our mixture model using 15 components. Each ellipse (except that of the 15th component) is shaded with the posterior mean of ρ_r for that component. The greater downtown and coastal regions exhibit stronger low-order serial dependence and daily seasonality.

computed by our mixture model with 15 components and averaged across the last 25,000 Monte Carlo samples. Note that the demand is, perhaps not surprisingly, very concentrated at the heart of downtown during working hours in the day, but is more spread out at various places in Toronto during the night. Figure 4 show the posterior log spatial densities using variable numbers of components around Wednesday midnight; these spatial densities are similar to that using 15 components (shown in Figure 3 (b)).

5 Model Performance and Validation

We evaluate the performance and validity of our models in several ways. For performance, we attempt to predict ambulance demand on two sets of test data (March 2007 and February 2008). To do this using mixture models, we train our models on data from February 2007, and use the resulting density estimates to predict for both sets of test data. We introduce in Section 5.1 two methods for comparisons. We compare the statistical predictive accuracies for all methods in Section 5.2. We then, in Section 5.3, put these predictive accuracies in the context of EMS

operations. We verify the validity of our method in Section 5.4.

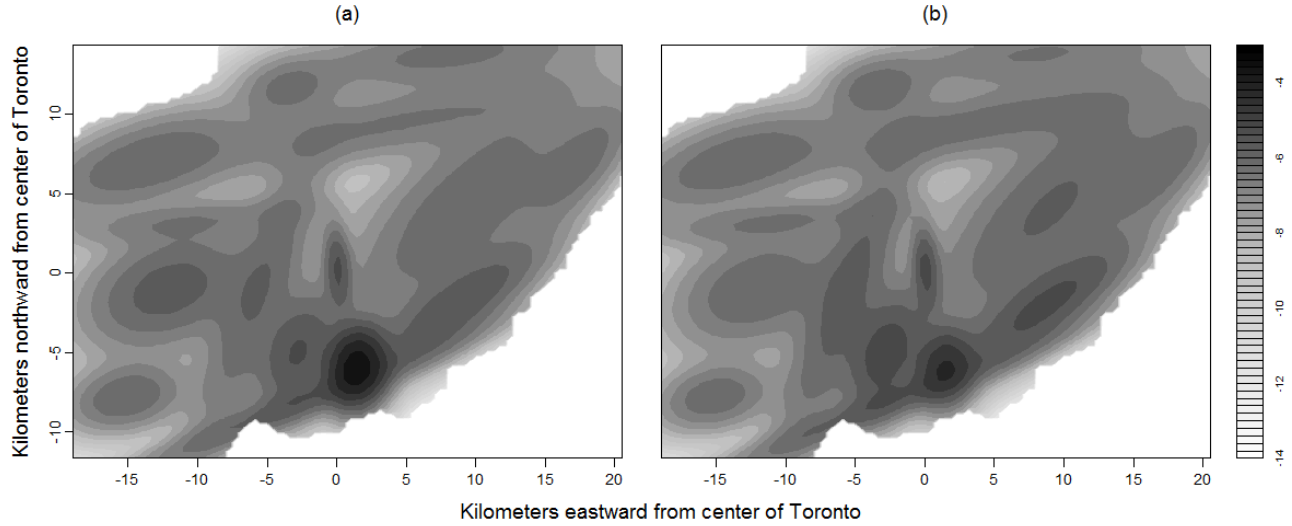


Figure 3: Fitting proposed mixture model using 15 components: (a) posterior log spatial density for Wednesday 2-4pm (demand concentrated at downtown during the day); (b) posterior log spatial density for Wednesday 2-4am (demand more spread out during the night).

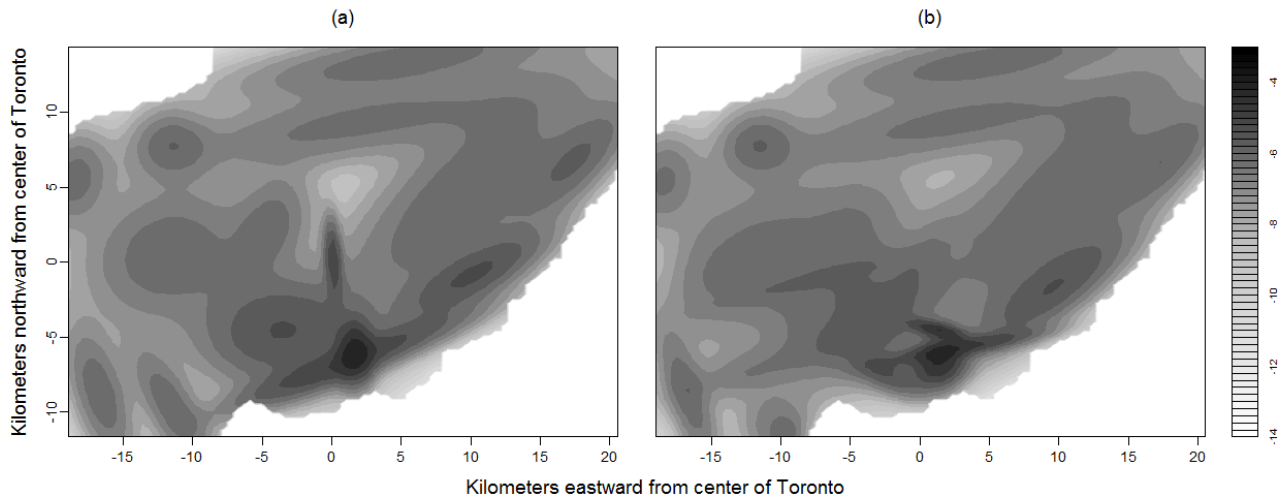


Figure 4: Fitting proposed mixture model using variable number of components: (a) posterior log spatial density for Wednesday 2-4am (night) using an average of 19 components; (b) that using an average of 24 components.

5.1 Comparison Methods

We compare our proposed mixture models to a current industry practice, and to a modified version of the industry practice that uses kernel density estimation (KDE). Toronto EMS currently employs an averaging method based on a discretized spatial and temporal domains. The demand

forecast at a spatial cell in a particular time period is the average of four corresponding realized demands for the past four years (from the same location, week of the year, day of the week, and hour of the day). Each spatial cell is 1 kilometer by 1 kilometer. A similar practice described in Setzler et al. (2009), the MEDIC method, uses the average of up to twenty corresponding historical demands in the preceding four weeks, for the past five years. These industry practices capture, to various extents, yearly and weekly seasonalities present in EMS demand.

We implement the MEDIC method as far as we have historic data available. Since we focus on predicting the demand density, we normalize demand volumes at any place by the total demand for the time period. For any 2-hour period in March 2007, we average the corresponding demand densities in the preceding four weeks. For any 2-hour period in February 2008, we average the corresponding demand densities in the preceding four weeks in 2008 and those same four weeks in 2007. For example, to forecast the demand density for 8-10am on the second Monday of February 2008, we average the demand densities at 8-10am in the first Monday of February 2008, the last three Mondays of January 2008, the first Monday of February 2007 and the last three Mondays of January 2007. Note that this means the MEDIC method is trained on at least as much data, which is at least as recent as that used in the mixture models. We adopt the same 1-km-by-1-km spatial discretization used by Toronto EMS.

Since our method is continuous in space, we also extend the MEDIC method to predict continuous demand densities as our second comparison method. The demand density for each 2-hour period is taken to be the kernel density estimate for all observations from that period. Here we use a bivariate normal kernel function, and bandwidths chosen by cross validation using the predictive accuracy measure in Section 5.2. We predict demand densities for March 2007 and February 2008 by averaging past demand densities using the MEDIC rule described above.

Figure 5 shows the log predictive density using these two competing methods for February 6, 2008 (Wednesday) 2-4am. Compare these two densities with Figure 3(b) and 4, which are the log predictive densities for the same time period using our proposed mixture models. Compared to the proposed model, both the MEDIC and MEDIC-KDE produce somewhat noisy predictions.

To ensure fair comparisons, we numerically normalize predictive densities produced by our

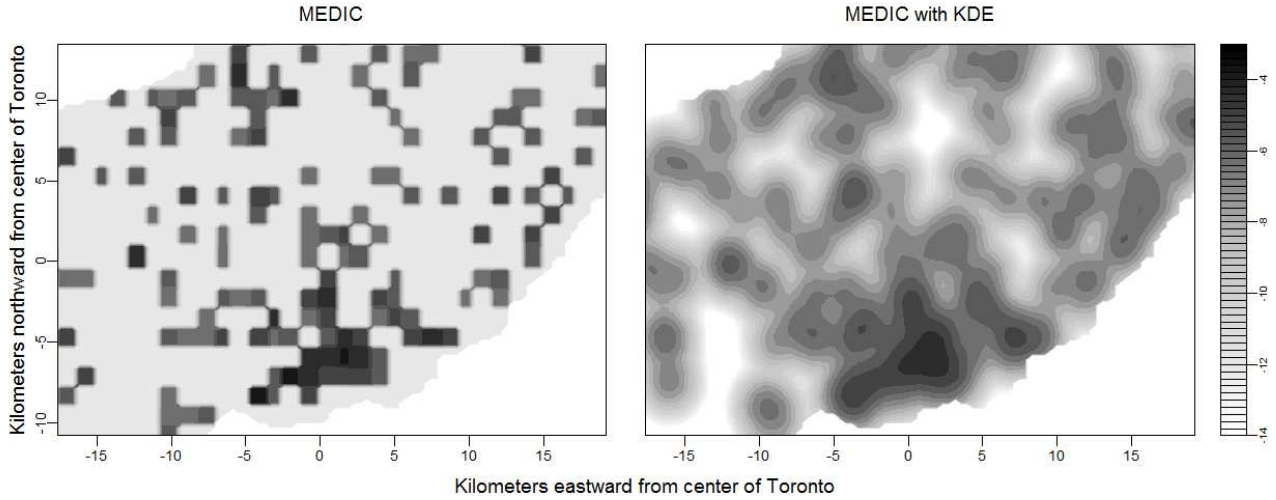


Figure 5: Log predictive densities using two current industry estimation methods for 2-4am (night) on February 6, 2008 (Wednesday). Figure 3(b) and Figure 4 show the log predictive densities for the same period using mixture models. Compared to mixture models, estimates from the MEDIC and MEDIC-KDE are overly noisy.

method and the two comparison methods with respect to Toronto’s boundary after estimations are done. As a result, we predict outside of Toronto’s boundary with probability zero, and the predictive accuracy within the boundary is elevated proportionally for each method. Note that we do not impose this boundary during estimation; doing so would be very computationally intensive because a numerical integration is needed for every Metropolis-Hastings proposal of μ_j and Σ_j at every time period.

5.2 Statistical Predictive Accuracy

To measure the predictive accuracy of density estimates obtained from our mixture models, MEDIC, and MEDIC-KDE, we use the average logarithmic score. First proposed by Good (1952), this performance measure is advocated for being a strictly proper scoring rule and its connections with Bayes factor and Bayes information criterion (Gneiting and Raftery, 2007). We define

$$\text{PA}(\{\tilde{\mathbf{s}}_{t,i}\}) = \frac{1}{\sum_{t=1}^T n_t} \sum_{t=1}^T \sum_{i=1}^{n_t} \log \hat{f}_t(\tilde{\mathbf{s}}_{t,i}), \quad (6)$$

in which $\hat{f}_t(\cdot)$ is the density estimate for time t obtained using various methods, and $\tilde{\mathbf{s}}_{t,i}$ represent the test data (March 2007 or February 2008). For the proposed mixture models, we use the Monte

Carlo estimate of Equation (6)

$$PA_{mix}(\{\tilde{\mathbf{s}}_{t,i}\}) = \frac{1}{M} \sum_{m=1}^M \left[\frac{1}{\sum_{t=1}^T n_t} \sum_{t=1}^T \sum_{i=1}^{n_t} \log \hat{f}_t(\tilde{\mathbf{s}}_{t,i} | \boldsymbol{\theta}^{(m)}) \right],$$

in which $\boldsymbol{\theta}^{(m)}$ represents the m th-iteration posterior parameter estimates generated from the training data, for $m \in \{1, \dots, M\}$ and some large M .

The predictive accuracies of various methods for two test data sets (March 2007 and February 2008) are shown in Table 1. The predictive accuracies for Gaussian mixture models are presented with their 95% consistent, nonoverlapping batch means confidence intervals (see Jones et al., 2006), which reflect the accuracy of the MCMC estimates. Here, a less negative predictive accuracy indicates better performance. Our proposed mixture models outperform the two current industry methods. Allowing for a variable number of components improves the predictive accuracy slightly. Since these marginal improvements come with extra computational costs, we conclude that our best model is the mixture model with a fixed number of components at 15.

Estimation method		PA for Mar 07	PA for Feb 08
Gaussian Mixture	15 components (§2)	-6.1378 ± 0.0004	-6.1491 ± 0.0005
	Variable number of comp (§3):		
	average 19 comp	-6.080 ± 0.002	-6.128 ± 0.002
	average 24 comp	-6.072 ± 0.003	-6.122 ± 0.004
Competing Methods	MEDIC	-8.31	-7.62
	MEDIC-KDE	-6.87	-6.56

Table 1: Predictive accuracies of proposed Gaussian mixture models and competing methods on test data of March 2007 and February 2008. The predictive accuracies for mixture models are presented with their 95% batch means confidence intervals.

5.3 Operational Predictive Accuracy

In this section, we quantify the advantage of our model over the current industry practice. We show that our proposed model gives much more accurate forecasts of the industry’s operational performance. The standard EMS operational performance measure is the fraction of calls with response times below various thresholds (e.g., 60% responded within 4 minutes). Obtaining an accurate forecast of this performance is of paramount importance because many aspects of the industry’s strategic management aim to optimize this performance. Accuracy in predicting this

performance depends crucially on the accuracy of spatio-temporal demand forecasts.

For each of the three methods of interest, we have a set of 2-hour demand density forecasts for March 2007 and February 2008. Using density forecasts generated by method \mathcal{M} for time period t , we predict the operational performance by computing the proportions of demand, $\mathcal{P}_{\mathcal{M},t}(r)$, reachable within response time threshold r from any of the 44 ambulance bases in Toronto (see Figure 5.3(a)). To do so, we first discretize Toronto into a very fine spatial grid and outline the regions that can be covered within any response time threshold. We then numerically integrate within these regions the demand density forecasts from \mathcal{M} , for each t and r , to obtain $\mathcal{P}_{\mathcal{M},t}(r)$. We also compute the realized performances using the test data, $\mathcal{P}_{test,t}(r)$. For simplicity, we assume ambulances always travel at the median speed of Toronto EMS trips, 46.44 kilometers / hour. We also take L_1 (Manhattan) distance between any base and any location. We consider response time thresholds ranging from 60 seconds to 300 seconds at 10-second intervals.

We compute the average absolute error in predicting operational performance made by each method under various response time thresholds, as compared to the truth. We define $\text{Error}(\mathcal{M}, r) = \frac{1}{T} \sum_{t=1}^T |\mathcal{P}_{\mathcal{M},t}(r) - \mathcal{P}_{test,t}(r)|$. In Figure 6 (b) and (c), we show $\text{Error}(\mathcal{M}, r)$ against r for each method \mathcal{M} (mixture model with 15 components, MEDIC, and MEDIC-KDE), using test data from March 2007 and February 2008, respectively. The 95% confidence bands for $\text{Error}(\mathcal{M}, r)$ are shown in gray; these bands indicate interval estimates for the average absolute errors for each \mathcal{M} and r given a time series of errors. We find that our method predicts the operational performance much more accurately, given the same set of operational assumptions about base locations, speed and distance. Our method reduces error by as much as two-thirds compared to the MEDIC method, despite sometimes using less recent training data. We expect similar orderings of the three methods under different sets of operational strategies.

5.4 Model Validation

We assess the goodness-of-fit of our models and the validity of our NHPP assumption. We use the model checking approach by Taddy and Kottas (2012), where each marginal of the point event data is transformed into quantities that are assumed to be uniformly distributed, and compared to

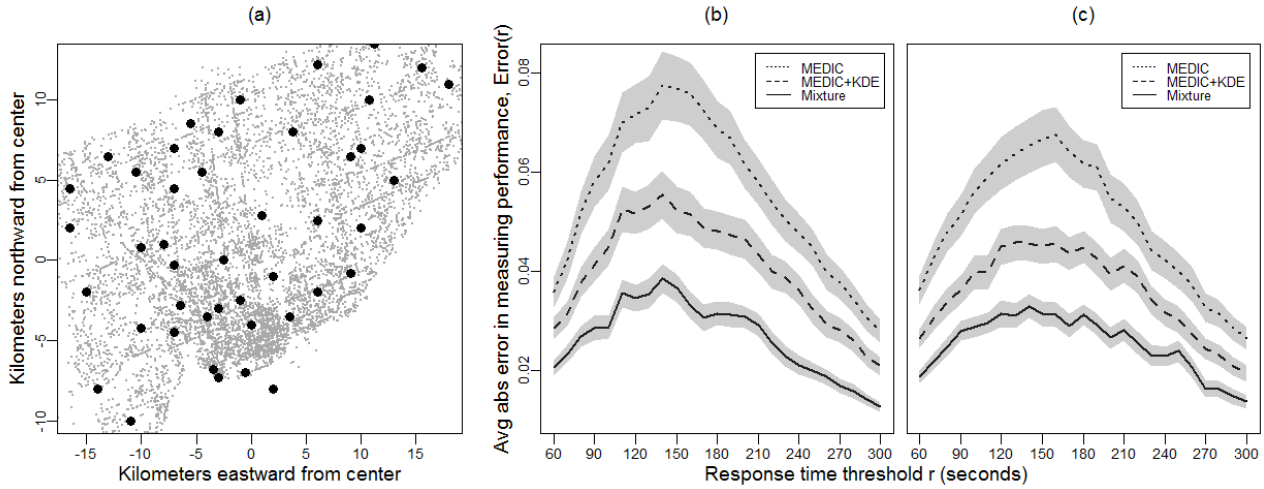


Figure 6: (a) all 44 ambulance bases in Toronto; (b) and (c) average absolute error in measuring operational performance made by our mixture model (15 components), MEDIC, and MEDIC-KDE, using test data from March 2007 and February 2008, respectively (with 95% confidence intervals in gray). Our mixture model outperforms the competing methods.

the true uniform distribution graphically. In particular, we have assumed that our point process follows a NHPP with time-varying intensity $\lambda_t(\mathbf{s}) = \delta_t f_t(\mathbf{s})$. We have posterior estimates of $\{f_t(\mathbf{s})\}$ from our proposed mixture models, and since we do not estimate δ_t , we assume that $\delta_t = n_t$, where n_t is the total number of observations in the t -th period. Point locations along the first and the second spatial dimension thus follow one-dimensional NHPP with marginalized intensities of $\lambda_t(\cdot)$, denoted as $\lambda_{1,t}(\cdot)$ and $\lambda_{2,t}(\cdot)$ respectively. We compute the corresponding cumulative intensities $\Lambda_{1,t}(\cdot)$ and $\Lambda_{2,t}(\cdot)$ and sort the observations for each time period into ordered marginals $\{\bar{s}_{j,1}, \dots, \bar{s}_{j,n_t}\}$ for each dimension $j \in \{1, 2\}$. If our assumptions are valid and our models have perfect goodness-of-fit, then $\{\Lambda_{j,t}(\bar{s}_{j,i}) : i = 1, \dots, n_t\}$ for each t and $j \in \{1, 2\}$ follows a homogeneous Poisson process with unit rate, and $u_{i,j,t} = 1 - \exp\{-(\Lambda_{j,t}(\bar{s}_{j,i}) - \Lambda_{j,t}(\bar{s}_{j,i-1}))\}$ for $i \in \{1, \dots, n_t\}$, $j \in \{1, 2\}$ and $t \in \{1, \dots, T\}$ are i.i.d uniform random variables on $(0,1)$. We compare the $u_{i,j,t}$ samples obtained from our models with the uniform distribution via quantile-quantile (Q-Q) plots. We have a set of $\{u_{i,j,t}\}$ for each set of posterior parameter estimates. In Figure 7 we show the mean Q-Q line and the 95% bounds reflecting this uncertainty in MCMC sampling. All three plots indicate high goodness-of-fit, whether we are using a fixed or a variable number of components.

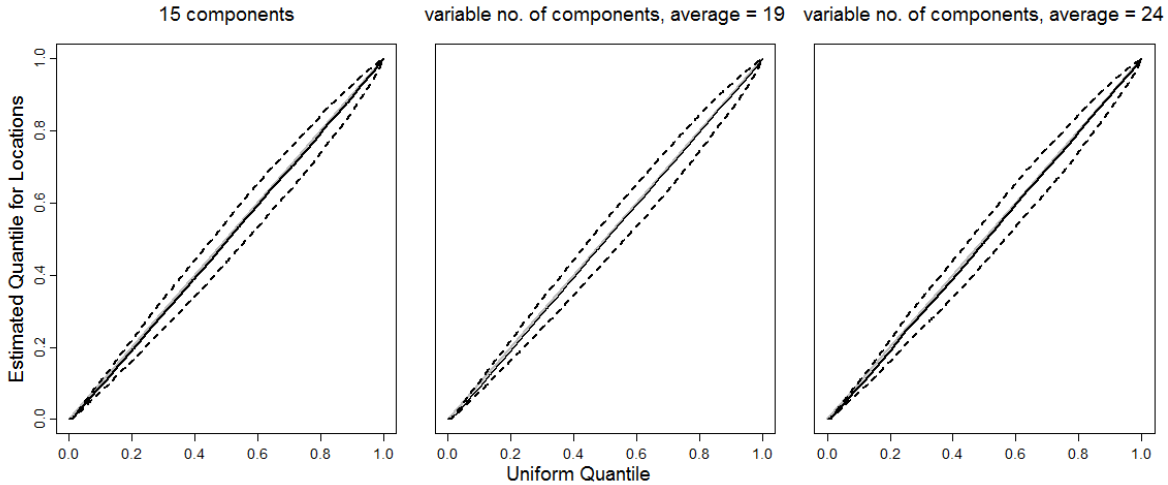


Figure 7: Posterior Q - Q plots for locations using our mixture models, where the solid lines show the posterior mean Q - Q lines and the dash lines are the 95% posterior intervals. All three plots show that our models are adequate and appropriate.

6 Conclusions

We have presented a flexible and parsimonious method to model spatio-temporal ambulance demand in Toronto using finite mixture models, capturing the complex temporal patterns and dynamics in this large-scale dataset. We have quantified the statistical and operational merits of our method over current industry practice; we have provided a much-needed method for accurate ambulance demand estimation on fine time and location scales.

We have also developed a set of easily generalizable tools to achieve information sharing across time and space, and describe complex spatial and temporal characteristics in a point process. We jointly estimate mixture component distributions over time to promote efficient learning of spatial structures, and represent the temporal process effectively using mixture weights. This approach should apply to a wide range of settings in which particular spatial aspects of the point process are time invariant, or data are too sparse at the desired temporal granularity to describe spatial structures well. Translating the spatio-temporal process into an evolution of mixture weights provides a flexible and simple framework to explore diverse temporal patterns, dynamics, and their interactions with space. By constraining the mixture weights, we can capture strong temporal seasonalities and commonalities. By imposing autoregressive priors on the mixture weights, we can describe location-specific temporal dynamics with a rich dependence structure.

We have also shown that estimation can be implemented with a variable number of components.

Acknowledgments

The authors sincerely thank Toronto EMS for sharing their data. This research was partially supported by NSF Grant CMMI-0926814, NSF Grant DMS-1209103 and NSF Grant DMS-1007478.

References

- Besag, J. E. (1974), “Spatial interaction and the statistical analysis of lattice systems,” *Journal of the Royal Statistical Society, Series B*, 36, 192–225.
- Besag, J., York, J. C., and Mollié, A. (1991), “Bayesian image restoration, with two applications in spatial statistics (with discussion),” *Annals of the Institute of Statistical Mathematics*, 43, 1–59.
- Chakraborty, A., and Gelfand, A. E. (2010), “Analyzing spatial point patterns subject to measurement error,” *Bayesian Analysis*, 5, 97–122.
- Channouf, N., L’Ecuyer, P., Ingolfsson, A., and Avramidis, A. (2007), “The application of forecasting techniques to modeling emergency medical system calls in Calgary, Alberta,” *Health Care Management Science*, 10, 25–45.
- Diggle, P. J. (2003), *Statistical Analysis of Spatial Point Patterns*, second edn, London: Arnold.
- Ding, M., He, L., Dunson, D., and Carin, L. (2012), “Nonparametric Bayesian segmentation of a multivariate inhomogeneous space-time Poisson process,” *Bayesian Analysis*, 7, 235–262.
- Flegal, J. M., Haran, M., and Jones, G. L. (2008), “Markov chain Monte Carlo: Can we trust the third significant figure?,” *Statistical Science*, 23, 250–260.
- Gneiting, T., and Raftery, A. (2007), “Strictly proper scoring rules, prediction, and estimation,” *Journal of the American Statistical Association*, 102, 359–378.
- Good, I. J. (1952), “Rational decisions,” *Journal of the Royal Statistical Society: Series B*, 14, 107–114.
- Illian, J. B., Penttinen, A., Stoyan, H., and Stoyan, D. (2008), *Statistical Analysis and Modelling of Spatial Point Patterns*, Chichester, England: Wiley.
- Ji, C., Merl, D., and Kepler, T. B. (2009), “Spatial mixture modeling for unobserved point processes: Examples in immunofluorescence histology,” *Bayesian Analysis*, 4, 297–315.
- Jones, G. L., Haran, M., Caffo, B. S., and Neath, R. (2006), “Fixed-width output analysis for Markov chain Monte Carlo,” *Journal of the American Statistical Association*, 101, 1537–1547.
- Knorr-Held, L., and Besag, J. (1998), “Modelling risk from a disease in time and space,” *Statistics in Medicine*, 17, 2045–2060.
- Kottas, A., and Sansó, B. (2007), “Bayesian mixture modeling for spatial Poisson process intensities, with applications to extreme value analysis,” *Journal of Statistical Planning and Inference*, 137, 3151–3163.
- Matteson, D. S., McLean, M. W., Woodard, D. B., and Henderson, S. G. (2011), “Forecasting emergency medical service call arrival rates,” *Annals of Applied Statistics*, 5, 1379–1406.

- Møller, J., and Waagepetersen, R. P. (2004), *Statistical Inference and Simulation for Spatial Point Processes*, London: Chapman & Hall/CRC.
- Richardson, S., and Green, P. (1997), “On Bayesian analysis of mixtures with an unknown number of components (with discussion),” *Journal of the Royal Statistical Society: Series B*, 59, 731–792.
- Setzler, H., Saydam, C., and Park, S. (2009), “EMS call volume predictions: A comparative study,” *Computers & Operations Research*, 36, 1843–1851.
- Stephens, M. (2000), “Bayesian analysis of mixture models with an unknown number of components - an alternative to reversible jump methods,” *Annals of Statistics*, 28, 40–74.
- Taddy, M. A. (2010), “Autoregressive mixture models for dynamic spatial Poisson processes: Application to tracking intensity of violent crime,” *Journal of the American Statistical Association*, 105, 1403–1417.
- Taddy, M. A., and Kottas, A. (2012), “Mixture modeling for marked Poisson processes,” *Bayesian Analysis*, 7, 335–362.
- Vile, J. L., Gillard, J. W., Harper, P. R., and Knight, V. A. (2012), “Predicting ambulance demand using singular spectrum analysis,” *Journal of the Operations Research Society*, 63, 1556–1565.